

# Anisotropic escape mechanism and elliptic flow of bottomonia

Partha Pratim Bhaduri,<sup>1</sup> Nicolas Borghini,<sup>2</sup> Amaresh Jaiswal,<sup>3</sup> and Michael Strickland<sup>4</sup>

<sup>1</sup>*Variable Energy Cyclotron Centre, HBNI, 1/AF Bidhan Nagar, Kolkata 700 064, India*

<sup>2</sup>*Fakultät für Physik, Universität Bielefeld, Postfach 100131, D-33501 Bielefeld, Germany*

<sup>3</sup>*School of Physical Sciences, National Institute of Science Education and Research, HBNI, Jatni-752050, India*

<sup>4</sup>*Department of Physics, Kent State University, Kent, OH 44242 United States*

(Dated: July 22, 2022)

We study the role of anisotropic escape in generating the elliptic flow of bottomonia produced in ultrarelativistic heavy-ion collisions. We implement temperature-dependent decay widths for the various bottomonium states, to calculate their survival probability when traversing through the anisotropic hot medium formed in non-central collisions. For the latter, we use initial conditions from a Glauber model and mimic the transverse expansion of the fireball in an effective way, assuming longitudinal boost invariance. We provide the first quantitative prediction for bottomonium elliptic flow generated from an anisotropic escape mechanism.

## I. INTRODUCTION

Heavy quarks, such as charm ( $c$ ) and bottom ( $b$ ) quarks, and their quarkonium bound states ( $c\bar{c}$  and  $b\bar{b}$ ) are very useful internal probes of the hot and dense medium created in collisions of heavy nuclei at high energies [1]. Heavy quarkonia created in high-energy collisions at the BNL Relativistic Heavy Ion Collider (RHIC) and the CERN Large Hadron Collider (LHC) have been found to be appreciably affected by the medium. This leads to distinctive features in their observed final yields, which encode information about the thermodynamic and transport properties of the medium. Therefore understanding the dynamics of heavy quarks and quarkonia in a deconfined medium is of great interest for the heavy-ion physics community [1–8].

In the classical picture [2, 3], heavy quarkonia embedded in a static, equilibrated quark-gluon plasma (QGP) may survive at temperatures above the QGP crossover temperature due to their large binding energies. However, if the QGP energy density becomes sufficiently high, the resulting Debye screening of the quark-antiquark potential eventually leads to the dissociation of charmonia and bottomonia [2, 3]. In this classical picture, the bound states with the largest binding energy, respectively the  $J/\psi$  and the  $\Upsilon$ , have the highest dissociation temperatures.

In recent years, this simple picture has been challenged by a number of findings. Based on first-principles finite-temperature quantum chromodynamics (QCD) calculations, it was shown that the in-medium quark-antiquark potential contains an imaginary part which is associated with the in-medium quarkonium breakup rate [9, 10]. This results in significant thermal widths for quarkonia, at variance with the older assumption of uniquely defined binding energies, and leads to the suppression of quarkonia at temperatures at which they would survive in the traditional scenario [11–14].

Another extension to the standard idea is the introduction of dynamics. In the dynamical picture, quarkonium states are both dissociated and (re-)associated with the

rate for each process depending on the open heavy flavor density and temperature of the system [16, 17]. In particular, in an evolving QGP with decreasing temperature, a quark and an antiquark pair may combine into a stable bound state which was until then unstable [18, 19]. For the fireball created in heavy-ion collisions at RHIC or LHC, recombination seems to be marginal for bottomonia [20, 21] while playing a more important role in the observed yields of charmonia [22]. In this paper we will investigate bottomonia, whose dynamical evolution is not significantly affected by regeneration, due to the fact that  $b\bar{b}$  pairs are less abundantly produced by initial hard scatterings than  $c\bar{c}$  pairs.

An additional important aspect of the dynamics is that the dissociation process is not instantaneous, but depends on how long the quark-antiquark pairs experience a high medium energy density. This is irrelevant in a static infinite QGP, but becomes important in an expanding finite-sized fireball. In that case, and for pairs in motion relative to the QGP, this translates into a dependence on the in-medium path length of the pairs. Thus, the bound states created in a high energy heavy-ion collision that survive the ensuing immersion in the fireball are those that quickly reach a region of low enough temperature. This path-length dependence of the bound-state survival probability is naturally described within an “escape mechanism” scenario [23–26]. Since a generic heavy-ion collision gives rise to a spatially anisotropic overlap in the plane transverse to the beam axis, the path-length dependence of states propagating through the generated QGP results in an anisotropic emission pattern of the quarkonia, measured in momentum space, as was first predicted for  $J/\psi$  [27]. For bottomonia, the anisotropic escape probability should constitute the major ingredient to the observed momentum anisotropy, quantified as usual in terms of Fourier harmonics  $v_n$ .

In this paper, we provide the first quantitative prediction for bottomonium elliptic flow  $v_2$  generated by the anisotropic escape mechanism; for a qualitative discussion, see Ref. [28]. We introduce in Sec. II a model fireball, which mimics in an effective way the expansion of that created in mid-central Pb+Pb collisions

at  $\sqrt{s_{\text{NN}}} = 2.76$  TeV at the LHC. For the bottomonium states, we implement temperature-dependent decay widths and calculate their resulting survival probability in the hot and dense anisotropic medium in Sec. III. Including the feed down contribution to the bottomonium ground state from higher excited states, we find that the elliptic flow of the  $\Upsilon(1S)$  is at the level of a few percent and investigate its dependence on the parameters governing the medium expansion in Sec. IV.

## II. FIREBALL EXPANSION

Since our purpose is to investigate the efficiency of the anisotropic escape mechanism at generating bottomonium flow, we employ a simplified model of the fireball, in which we can modify some of the parameters governing the expansion at will, instead of using more realistic fluid-dynamical events.

The starting point for the model is an initial energy density distribution in the transverse plane. For the longitudinal expansion, we consider boost-invariant flow, i.e.  $v^z = z/t$ . Accordingly, we work in the Milne coordinate system  $(\tau, x, y, \eta_s)$ , where  $\tau = \sqrt{t^2 - z^2}$  and  $\eta_s = \tanh^{-1}(z/t)$ . Due to boost invariance, the system evolution is independent of  $\eta_s$  and therefore from now on it will no longer appear in our calculations. For a point  $(x, y)$  in the transverse plane, we shall also use the notation  $\mathbf{r}$  or polar coordinates  $(r, \theta)$  with  $r = |\mathbf{r}|$ . In what follows, we will assume an ideal equation of state.

In the absence of transverse expansion, longitudinal boost invariance results in the well-known Bjorken scaling solution and every point  $(x, y)$  [29]

$$\varepsilon(x, y, \tau) = \varepsilon(x, y; \tau_i) \left( \frac{\tau}{\tau_i} \right)^{-4/3} \quad (1)$$

with  $\tau_i$  the initial proper time at which we specify the energy density. This behavior will be modified to account for the transverse expansion in an effective way.

If the transverse expansion were purely radial, then the medium which is at  $x_i = r_i \cos \theta$ ,  $y_i = r_i \sin \theta$  at the initial time  $\tau_i$  is further away from the origin at later times, say at

$$x(\tau) = r(\tau) \cos \theta \quad , \quad y(\tau) = r(\tau) \sin \theta \quad (2)$$

with  $r(\tau_i) = r_i$ . Such a purely radial transverse expansion is admittedly not realistic, but makes things simpler for this first analysis. In particular, it leads to a  $\tau$ -dependence of the transverse shape of the system, quantified for instance by eccentricity coefficients  $\varepsilon_n$ , unless one starts with a  $\theta$ -independent energy-density profile. Building this radial transverse motion into the Bjorken solution (1), we shall assume

$$\varepsilon(x(\tau), y(\tau); \tau) = \varepsilon(x_i, y_i; \tau_i) \left( \frac{\tau}{\tau_i} \right)^{-4/3} \quad (3)$$

for the evolution of the energy density, with the interpretation that what one finds at  $x(\tau)$ ,  $y(\tau)$  at time  $\tau$  was originally at  $x_i = x(\tau_i)$ ,  $y_i = y(\tau_i)$ , and taking also into account the dilution from longitudinal expansion. This ansatz for the energy density is not a valid solution of the fluid-dynamical equations, but it captures the necessary features of the dynamics necessary to estimate the magnitude of the anisotropic escape of quarkonia states.

We now need to specify the (radial) transverse velocity profile of the medium. We assume that it grows with  $\tau$  and parametrize it as

$$\beta_T(\tau, r) = [\beta_0(\tau) + 2\beta_2(\tau) \cos 2\theta] \frac{r}{R_0}, \quad (4)$$

where  $R_0$  is a typical scale like the initial nuclear radius. For the functions encoding the time dependence of the transverse velocity profile, we take

$$\beta_0(\tau) = b_0 \left( \frac{\tau - \tau_i}{\tau_i} \right)^{n_0}, \quad \beta_2(\tau) = b_2 \left( \frac{\tau - \tau_i}{\tau_i} \right)^{n_2}. \quad (5)$$

For later purposes it is convenient to introduce  $\tau' \equiv \tau - \tau_i$ , in which case we shall simply write  $r(\tau')$ ,  $\beta_0(\tau')$ ,  $\beta_2(\tau')$ , and so on. Note that our velocity profile vanishes at  $\tau = \tau_i$ , i.e.  $\tau' = 0$ : that is, we assume no “pre-flow” in the system. The values of  $b_0$  and  $b_2$  in Eq. (5) are tuned to match the blast wave fitted values of  $\beta_0^{\text{BW}} = \beta_0(\tau_f^{\text{BW}})$  and  $\beta_2^{\text{BW}} = \beta_2(\tau_f^{\text{BW}})$ , where  $\tau_f^{\text{BW}}$  can be taken to be the freeze-out time of the central cell. This leads to the relations

$$b_0 = \beta_0^{\text{BW}} \left( \frac{\tau_i}{\tau_f'} \right)^{n_0}, \quad b_2 = \beta_2^{\text{BW}} \left( \frac{\tau_i}{\tau_f'} \right)^{n_2}, \quad (6)$$

where  $\tau_f' \equiv \tau_f^{\text{BW}} - \tau_i$ . In the present calculations, unless otherwise mentioned, we have taken  $\beta_0^{\text{BW}} = 0.6$  and  $\beta_2^{\text{BW}} = 0.06$ . Using the fact that  $\beta_T(\tau', r) = dr/d\tau'$ , we integrate with appropriate limits to obtain

$$r_i = r(\tau') \exp \left[ - \left( \frac{\beta_0(\tau')}{n_0 + 1} + \frac{2\beta_2(\tau')}{n_2 + 1} \cos 2\theta \right) \frac{\tau'}{R_0} \right], \quad (7)$$

where for reasons that will become clearer in the next section we express  $r_i$  in terms of  $r(\tau')$ , instead of the other way round. To start with, we assume the time evolution of  $\beta_0$  and  $\beta_2$  to be linear, i.e.  $n_0 = n_2 = 1$ .

## III. DECAY WIDTH AND SURVIVAL PROBABILITY OF BOTTOMONIA

Let us now turn to the description of the production of bottomonia and their behavior in the QGP. The bottomonium states are produced in initial hard scattering processes during the very earliest stages of the heavy-ion collision. The spatial distribution of the production points in the transverse plane is assumed to follow that of the number of binary collisions,  $N_{\text{coll}}(x, y)$ . We assume a

power-law transverse momentum ( $p_T$ ) distribution of the  $\Upsilon$ 's obtained from PYTHIA simulations for  $p + p$  collisions, scaled by the mass number of the colliding nuclei. Note that this kind of scaling implicitly assumes that the bottomonia do not “flow” with the medium and any  $v_2$  that we obtain in our model will be purely due to the anisotropic escape mechanism. The initial  $\Upsilon$  distribution for  $p + p$  collision is assumed to be given by [30]

$$\frac{d^2\sigma_{\Upsilon}^{pp}}{p_T dp_T dY} = \frac{4}{3\langle p_T^2 \rangle_{pp}} \left(1 + \frac{p_T^2}{\langle p_T^2 \rangle_{pp}}\right)^{-3} \frac{d\sigma_{\Upsilon}^{pp}}{dY}, \quad (8)$$

with  $Y$  being the longitudinal rapidity in momentum space. Here  $\langle p_T^2 \rangle_{pp}(Y) = 20(1 - Y^2/Y_{\max}^2)$  (GeV/c)<sup>2</sup>, where  $Y_{\max} = \cosh^{-1}(\sqrt{s_{NN}}/(2m_{\Upsilon}))$  is the most forward rapidity of the bottomonia. Eventually, the momentum rapidity density follows a Gaussian distribution:

$$\frac{d\sigma_{\Upsilon}^{pp}}{dY} = \frac{d\sigma_{\Upsilon}^{pp}}{dY} \Big|_{Y=0} e^{-Y^2/0.33Y_{\max}^2}. \quad (9)$$

For our calculations, we integrate over  $Y$  and consider the resulting  $p_T$  distribution.

The formation of each bound bottomonium state requires a finite formation time  $\tau_{\text{form}}$ . The value  $\tau_{\text{form}}^0$  of the latter in the bottomonium rest frame is assumed to be proportional to the inverse of the vacuum binding energy for each state. For the  $\Upsilon(1S)$ ,  $\Upsilon(2S)$ ,  $\Upsilon(3S)$ ,  $\chi_b(1P)$  and  $\chi_b(2P)$  states we use  $\tau_{\text{form}}^0 = 0.2, 0.4, 0.6, 0.4, 0.6$  fm/c, respectively [14]. In the laboratory frame, relative to which a bottomonium state with mass  $M$  has transverse momentum  $p_T$ , the formation time becomes  $\tau_{\text{form}} = E_T \tau_{\text{form}}^0 / M$  with  $E_T = \sqrt{p_T^2 + M^2}$  being the transverse energy.

After they are formed, since the bound  $b\bar{b}$  states are color-neutral, their elastic scatterings on the color charges in the QGP are fewer and, because of their large rest mass, they propagate quasi freely, following nearly straight-line trajectories. If  $(x_0, y_0)$  denotes the position in the transverse plane where a bottomonium with momentum  $p_T$  is at time  $\tau_i$ , it will at a later time  $\tau = \tau_i + \tau'$  be at

$$x' = x_0 + v_T \tau' \cos \phi, \quad y' = y_0 + v_T \tau' \sin \phi, \quad (10)$$

where  $v_T = p_T/E_T$  is the bottomonium transverse velocity and  $\phi$  the azimuthal angle of its transverse momentum. Introducing now the polar coordinates  $(r', \theta)$  of  $(x', y')$ ,

$$r' \cos \theta = x_0 + v_T \tau' \cos \phi, \quad r' \sin \theta = y_0 + v_T \tau' \sin \phi, \quad (11)$$

where the radial coordinate is

$$r' = \sqrt{(x_0 + v_T \tau' \cos \phi)^2 + (y_0 + v_T \tau' \sin \phi)^2} \equiv r(\tau'), \quad (12)$$

we can invoke Eq. (7) to determine the initial position at  $\tau' = 0$  of the piece of medium which is at  $(x', y')$  at  $\tau'$ , and thus the medium energy density  $\varepsilon(x', y', \tau')$  experienced

by the  $b\bar{b}$  pair [Eq. (3)]. We use an ideal equation of state to translate this energy density into a local temperature  $T(x', y', \tau')$ .

With this temperature, we compute the thermal decay widths of the bottomonium states, adopting the recent state-of-the-art estimations of in-medium dissociation of different bound  $b\bar{b}$  states [11], which are here considered for the case of a locally momentum-isotropic medium for simplicity. For a given bound state, the 3-D Schrödinger equation is solved numerically with a temperature-dependent complex heavy-quark potential [15]. The in-medium breakup rates for each state are then computed from the imaginary part of the binding energy as a function of the temperature  $T/T_c$ . We then set the temperature scale to  $T_c = 160$  MeV. Below  $T_c$ , we assume that plasma screening effects are rapidly diminished due to transition to the hadronic phase and the widths of the states becoming approximately equal to their vacuum widths which in comparison to the in-medium widths are essentially zero.

The thermal decay rate  $\Gamma(T(x', y', \tau'))$  for a given state determines its survival probability as it propagates in the medium. For a bottomonium with transverse momentum  $p_T$  along the azimuthal  $\phi$  direction, which is created at position  $(x, y)$  at the formation time  $\tau_{\text{form}}$ , the final transmittance for a  $b\bar{b}$  bound state labelled by  $j$  is given by [11–14]

$$\mathcal{T}_j(x, y, p_T, \phi) = \exp \left[ -\Theta(\tau_f - \tau_j^{\text{form}}) \times \int_{\max(\tau_j^{\text{form}}, \tau_i)}^{\tau_f} d\tau' \Gamma_j \left( T(x', y'; \tau') \right) \right], \quad (13)$$

where  $\Theta$  is the usual step function. The final time  $\tau_f$  in the above equation is self consistently determined in the simulation as the proper time when the local effective temperature of the medium becomes less than the freeze out temperature  $T_f = 130$  MeV.

Note that the above form (13) of the escape probability of the produced bottomonium could alternatively be written in the form of the Beer–Lambert law used in Ref. [26],  $\mathcal{T} = \exp(-\int n \sigma d\ell)$ . The propagation time  $\tau'$  clearly maps one-to-one to the in-medium path length  $\ell = v_T \tau'$ . In turn, the product of number density  $n$  of the system, dissociation cross section  $\sigma$ , and velocity  $v_T$  precisely give the rate of destruction  $\Gamma$  of the bottomonium state under consideration.

#### IV. RESULTS AND DISCUSSIONS

In this section, we numerically evaluate Eq. (13) to calculate the elliptic flow of bottomonia due to escape probability through a medium having an anisotropic shape. We consider Pb + Pb collisions at  $\sqrt{s_{NN}} = 2.76$  TeV in 40 – 50% centrality class which corresponds to an average impact parameter of 10.5 fm [31]. The energy den-

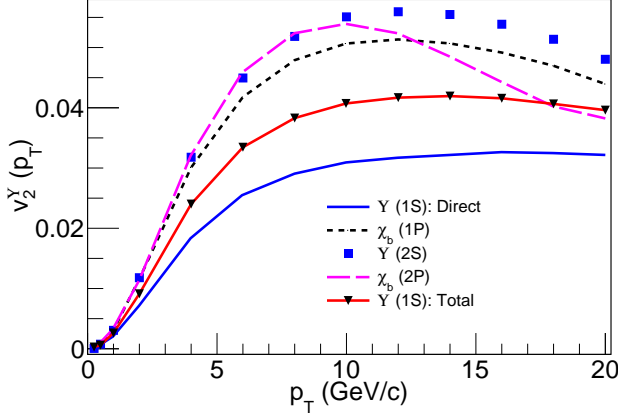


FIG. 1: Transverse momentum dependence of elliptic flow parameter for different bottomonium states with  $\beta_0^{\text{BW}} = 0.6$  and  $\beta_2^{\text{BW}} = 0.06$ . For  $\Upsilon(1S)$ , directly produced states and the inclusive yield including feed down contributions are shown.

sity in the transverse plane is generated from a Glauber model with Woods-Saxon nuclear density distribution, following a linear combination of the spatial profiles of the number of participant nucleons  $N_{\text{part}}$  and number of binary collisions  $N_{\text{coll}}$  as  $\varepsilon_i(x, y) \propto 0.85N_{\text{part}}(x, y) + 0.15N_{\text{coll}}(x, y)$  [11]. The inelastic nucleon-nucleon interaction cross section is taken to be  $\sigma_{NN} = 62$  mb and the initial energy density in the central cell of central Pb+Pb collisions at  $\tau_i = 0.4$  fm is taken to be 85 GeV/fm<sup>3</sup>, which corresponds to an initial temperature of 480 MeV.

In order to compare to the experimental results, we integrate over the entire temperature profile in the transverse plane, to obtain the weighted average “raw” spectra for each bottomonium state. To account for the post-QGP feed down of the excited states, we use a  $p_T$ -averaged feed down fraction obtained from a recent compilation of  $p + p$  data at LHC. The inclusive spectra for  $\Upsilon(1S)$  is then calculated from a linear superposition of the raw spectra for each state:

$$\frac{d^2 N_{\Upsilon(1S)}^{\text{all}}}{d^2 p_T} = \sum_i f_i \frac{d^2 N_i}{d^2 p_T}. \quad (14)$$

The contribution from different states are as follows:  $f_{2S \rightarrow 1S} = 8.6\%$ ,  $f_{3S \rightarrow 1S} = 1\%$ ,  $f_{1P \rightarrow 1S} = 17\%$ ,  $f_{2P \rightarrow 1S} = 5.1\%$  and  $f_{3P \rightarrow 1S} = 1.5\%$  as adopted from [14]. Since contribution from  $3S$  and  $3P$  states are small, we include their percentage contributions in  $2S$  and  $2P$  states, respectively. The inclusive spectra so constructed is then used to calculate the elliptic flow  $v_2$  of  $\Upsilon(1S)$ . Note that, while considering feed down, the transverse momentum of the mother and daughter bottomonium states are assumed to be the same. This assumption can be justified by considering the average  $p_T$  value of the mother excited states and the daughter  $1S$  states. Due to the large mass of the bottomonium states, we find that the mean  $p_T$  value of the mother excited states and the daughter  $1S$  states are almost identical.

The  $p_T$  dependence of  $v_2$  for different directly produced

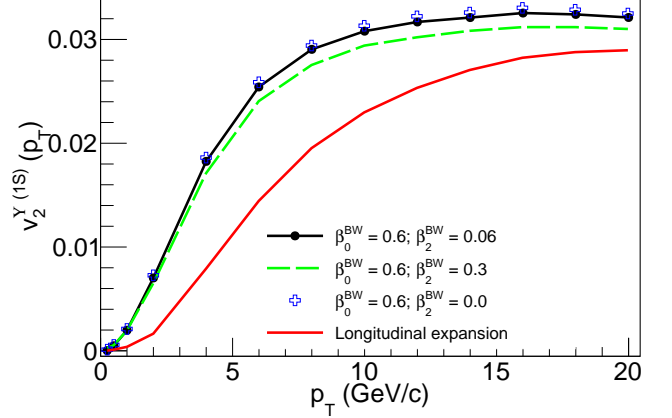


FIG. 2: Transverse momentum dependence of  $v_2$  of  $\Upsilon(1S)$  for different combinations of parameters for the medium expansion. The curve labeled “longitudinal expansion” corresponds to  $\beta_0^{\text{BW}} = \beta_2^{\text{BW}} = 0$ .

bottomonium states is shown in Fig. 1. For each state,  $v_2$  initially increases with  $p_T$  and gradually saturates. The inclusive  $v_2$  of the  $1S$  state which takes into account feed-down is also shown in the same plot. At a given  $p_T$ , owing to weaker binding and hence broader decay width,  $v_2$  is larger for the excited states, as was found in Ref. [20]. As nearly 30% of the measured  $\Upsilon(1S)$  come from the decay of excited states, inclusive  $v_2$  of  $1S$  is reasonably larger than that of directly produced  $1S$  states. At very high  $p_T \gtrsim 10$  GeV,  $v_2$  tends to decrease with increasing  $p_T$ , an effect which is more prominent for excited states. This reduction can be attributed to the competition between the dynamics of the plasma and that of the bottomonium state under consideration. Due to both its velocity as well as its dilated formation time in the plasma frame, a bottomonium with large  $p_T$  escapes faster from the plasma, spending less time inside and therefore the suppression effect is less important, leading to a reduced  $v_2$ .

In Fig. 2, we show  $v_2(p_T)$  for different combinations of the input parameters  $\beta_0^{\text{BW}}$  and  $\beta_2^{\text{BW}}$  controlling the medium expansion. Instead of considering all bottomonium states, we only report the directly produced  $1S$  states for this purpose. We find that a rather stronger  $v_2$  results as soon as transverse expansion of the medium is included, i.e. for  $\beta_0^{\text{BW}} \neq 0$ . However in presence of transverse expansion,  $v_2$  is much less sensitive to the parameter  $\beta_2^{\text{BW}}$ . Increasing  $\beta_2^{\text{BW}}$  leads to a decrease of  $v_2$ . This may be understood from the fact that, since the medium flow does not impart any  $v_2$  to bottomonium, increasing  $\beta_2^{\text{BW}}$  leads to a faster decrease of the spatial anisotropy of the medium and hence to a diminution of  $v_2$  generated from anisotropic escape.

## V. SUMMARY AND CONCLUSION

In this paper, we have provided the first quantitative prediction for the elliptic flow of bottomonia produced in

mid-central collisions in  $\sqrt{s_{NN}} = 2.76$  TeV Pb + Pb collisions at LHC via an anisotropic escape mechanism. We employed the Glauber model to generate initial distribution of energy density in the plane transverse to the beam axis. Using temperature-dependent decay widths for bottomonium states, we calculated their survival probability when traversing through the hot and dense anisotropic medium formed in non-central collisions. For the expansion of the fireball, we considered longitudinal Bjorken flow and a blast wave motivated effective expansion in the transverse plane. We also accounted for the feed down contribution to the bottomonium ground state from higher excited states. We found that the transverse momentum dependence of the elliptic flow of bottomonia is of the level of few percent, consistent with the finding of Ref. [20].

Looking forward, it will be interesting to consider the effect of medium-induced transitions between bound states which is predicted from the open quantum system approach [32–37]. In this “state reshuffling” scenario, transitions between various bound states become possible which counteracts the usual suppression picture by al-

lowing for the re-formation of otherwise suppressed states even above the hadronization temperature. Since the excited states of bottomonium acquire more elliptic flow due to anisotropic escape mechanism, one may expect to generate larger flow owing to the feed-down from excited states. Moreover, it is also important to perform the present analysis within a realistic hydrodynamic model. We leave these questions for future work.

## Acknowledgments

N.B. acknowledges support by the Deutsche Forschungsgemeinschaft (DFG) through the grant CRC-TR 211 “Strong-interaction matter under extreme conditions”. A.J. is supported in part by the DST-INSPIRE faculty award under Grant No. DST/INSPIRE/04/2017/000038. M.S. is supported by the U.S. Department of Energy, Office of Science, Office of Nuclear Physics under Award No. DE-SC0013470.

- 
- [1] A. Andronic *et al.*, Eur. Phys. J. C **76**, no. 3, 107 (2016) [arXiv:1506.03981 [nucl-ex]].
  - [2] T. Matsui and H. Satz, Phys. Lett. B **178**, 416 (1986).
  - [3] F. Karsch, M. T. Mehr and H. Satz, Z. Phys. C **37** 617, (1988).
  - [4] N. Brambilla *et al.* [Quarkonium Working Group], hep-ph/0412158.
  - [5] L. Kluberg and H. Satz, arXiv:0901.3831 [hep-ph].
  - [6] R. Rapp, D. Blaschke and P. Crochet, Prog. Part. Nucl. Phys. **65**, 209 (2010) [arXiv:0807.2470 [hep-ph]].
  - [7] H. van Hees, V. Greco and R. Rapp, Phys. Rev. C **73**, 034913 (2006) [nucl-th/0508055].
  - [8] H. van Hees and R. Rapp, Phys. Rev. C **71**, 034907 (2005) [nucl-th/0412015].
  - [9] M. Laine, O. Philipsen, P. Romatschke and M. Tassler, JHEP **0703**, 054 (2007) [hep-ph/0611300].
  - [10] A. Dumitru, Y. Guo and M. Strickland, Phys. Lett. B **662**, 37 (2008) [arXiv:0711.4722 [hep-ph]].
  - [11] M. Strickland and D. Bazow, Nucl. Phys. A **879**, 25 (2012) [arXiv:1112.2761 [nucl-th]].
  - [12] M. Strickland, Phys. Rev. Lett. **107**, 132301 (2011) [arXiv:1106.2571 [hep-ph]].
  - [13] B. Krouppa, R. Ryblewski and M. Strickland, Phys. Rev. C **92**, 061901 (2015) [arXiv:1507.03951 [hep-ph]].
  - [14] B. Krouppa and M. Strickland, Universe **2**, 16 (2016) [arXiv:1605.03561 [hep-ph]].
  - [15] M. Margotta, K. McCarty, C. McGahan, M. Strickland and D. Yager-Elorriaga, Phys. Rev. D **83**, 105019 (2011) Erratum: [Phys. Rev. D **84**, 069902 (2011)] [arXiv:1101.4651 [hep-ph]].
  - [16] L. Grandchamp, R. Rapp and G. E. Brown, Phys. Rev. Lett. **92**, 212301 (2004) [hep-ph/0306077].
  - [17] A. Emerick, X. Zhao and R. Rapp, Eur. Phys. J. A **48**, 72 (2012) [arXiv:1111.6537 [hep-ph]].
  - [18] R. L. Thews, M. Schroedter and J. Rafelski, Phys. Rev. C **63**, 054905 (2001) [hep-ph/0007323].
  - [19] P. Braun-Munzinger and J. Stachel, Phys. Lett. B **490**, 196 (2000) [nucl-th/0007059].
  - [20] X. Du, R. Rapp and M. He, Phys. Rev. C **96**, 054901 (2017) [arXiv:1706.08670 [hep-ph]].
  - [21] B. Krouppa, A. Rothkopf and M. Strickland, arXiv:1807.07452 [hep-ph].
  - [22] X. Zhao and R. Rapp, Phys. Rev. C **82**, 064905 (2010) [arXiv:1008.5328 [hep-ph]].
  - [23] N. Borghini and C. Gombeaud, Eur. Phys. J. C **71**, 1612 (2011) [arXiv:1012.0899 [nucl-th]].
  - [24] L. He, T. Edmonds, Z. W. Lin, F. Liu, D. Molnar and F. Wang, Phys. Lett. B **753**, 506 (2016) [arXiv:1502.05572 [nucl-th]].
  - [25] P. Romatschke, Eur. Phys. J. C **75**, 429 (2015) [arXiv:1504.02529 [nucl-th]].
  - [26] A. Jaiswal and P. P. Bhaduri, Phys. Rev. C **97**, 044909 (2018) [arXiv:1712.02707 [hep-ph]].
  - [27] X. N. Wang and F. Yuan, Phys. Lett. B **540**, 62 (2002) [nucl-th/0202018].
  - [28] D. Das and N. Dutta, Int. J. Mod. Phys. A **33**, 1850092 (2018) [arXiv:1802.00414 [nucl-ex]].
  - [29] J. D. Bjorken, Phys. Rev. D **27**, 140 (1983).
  - [30] K. Zhou, N. Xu and P. Zhuang, Nucl. Phys. A **931**, 654 (2014) [arXiv:1408.3900 [hep-ph]].
  - [31] B. Abelev *et al.* [ALICE Collaboration], Phys. Rev. C **88**, no. 4, 044909 (2013) doi:10.1103/PhysRevC.88.044909 [arXiv:1301.4361 [nucl-ex]].
  - [32] N. Borghini and C. Gombeaud, arXiv:1103.2945 [hep-ph].
  - [33] N. Borghini and C. Gombeaud, Eur. Phys. J. C **72**, 2000 (2012) [arXiv:1109.4271 [nucl-th]].
  - [34] Y. Akamatsu and A. Rothkopf, Phys. Rev. D **85**, 105011 (2012) [arXiv:1110.1203 [hep-ph]].
  - [35] N. Dutta and N. Borghini, Mod. Phys. Lett. A **30**, 1550205 (2015) [arXiv:1206.2149 [nucl-th]].

- [36] N. Brambilla, M. A. Escobedo, J. Soto and A. Vairo, Phys. Rev. D **96**, 034021 (2017) [arXiv:1612.07248 [hep-ph]].
- [37] J.-P. Blaizot and M. A. Escobedo, JHEP **1806**, 034 (2018) [arXiv:1711.10812 [hep-ph]].